Chapter 8

Intravital Microscopy and Its Application to Study Regulated Exocytosis in the Exocrine Glands of Live Rodents

Oleg Milberg, Natalie Porat-Shliom, Muhibullah Tora, Laura Parente, Andrius Masedunskas, and Roberto Weigert

Abstract

Regulated exocytosis is a fundamental event in specialized secretory organs that has been primarily studied in in vitro and ex vivo model systems. The recent application of intravital microscopy to image subcellular structures in vivo has enabled researchers to investigate the machinery controlling regulated exocytosis in live rodents. Here, we describe selected experimental models that have been used to investigate the dynamics of the secretory granules after their initial fusion their with the plasma membrane. Specifically, we used rodent salivary glands, an established model for exocrine secretion. Our goal is to provide the reader with guidelines on how to apply both qualitative and quantitative intravital microscopy to study regulated exocytosis and to highlight advantages and limitations of this approach.

Key words Regulated exocytosis, Exocrine glands, Actin cytoskeleton, Myosin, Intravital microscopy, Salivary glands

1 Introduction: Regulated Exocytosis in Exocrine Glands

Molecules destined for the cell surface are packed into membranous carriers that are transported to the cell periphery where they fuse with the plasma membrane and release their content into the extracellular space. This process is called exocytosis and can occur either in a constitutive or a regulated fashion [1–3]. Constitutive exocytosis occurs in every cell type and is fundamental for maintaining membrane homeostasis and cell polarity [4, 5]. On the other hand, regulated exocytosis occurs in specialized secretory cells and is elicited by extracellular stimuli that activate one or more receptors at the cell surface, which ultimately trigger an intracellular signaling cascade [6–8]. During regulated exocytosis transport intermediates are generated constitutively from intracellular

Peter Thorn (ed.), *Exocytosis Methods*, Neuromethods, vol. 83,
DOI 10.1007/978-1-62703-676-4_8,

organelles, such as the trans-Golgi network, and transported to the cell periphery where they accumulate under resting conditions [6–8]. Most of the stimuli elicit an increase in either intracellular Ca^{++} or cAMP that activates a series of processes which include the docking and the fusion of transport intermediates with the plasma membrane [6–8].

Regulated exocytosis occurs with different modalities and is regulated by various machineries depending on the secretory system. Indeed, secretory cells can be roughly divided in four categories: neuron, endocrine, hematopoietic, and exocrine. In the first three systems, molecules are transported in small vesicles (secretory vesicles that have diameters between 50 and 300 nm), which release their contents into the extracellular space, ultimately reaching the circulation [3, 9, 10]. In exocrine organs, molecules are stored in large vesicles (secretory granules that have diameters larger than 1 μm) and are released at specialized sites of the plasma membrane that form ductal structures which are in direct continuity with the external environment [1, 2]. After fusion, individual secretory granules remain connected to the extracellular space via the fusion pore that allows for their contents to be secreted. In some secretory systems, the membranes of the secretory granules are gradually integrated into the plasma membrane in a process that is coupled to the expansion of the fusion pore during the release of cargo molecules [11–13]. In other secretory systems, the fused secretory granules serve as docking and fusion sites for other secretory granules, which leads to the formation of strings of fused granules whose lumen is in continuity with the extracellular space (i.e., compound exocytosis) [11, 14, 15]. Regardless of the modalities of post-fusion events, the membranes of the secretory granules that are added to the plasma membrane are retrieved by the stimulation of endocytic events (i.e., compensatory endocytosis) [16–18].

The machinery controlling regulated exocytosis in exocrine glands has been extensively investigated by using three main models: pancreas, lacrimal glands, and salivary glands (SGs) [2, 19, 20]. Furthermore, several molecules have been identified to play fundamental roles in this process both in terms of signaling components and membrane regulators, such as Rab GTPase, lipid kinases, SNAREs, and the cytoskeleton [1]. The actin cytoskeleton, in particular, plays a fundamental role in controlling regulated exocytosis in exocrine glands, and several cytoskeletal components have also been shown to control both pre-fusion (docking, priming, and fusion) and post-fusion events (maintenance of the fusion pore, compound exocytosis, gradual collapse, and compensatory endocytosis) [2, 13, 19–22].

1.1 Methods to Study Regulated Exocytosis in Exocrine Glands

In exocrine glands, regulated exocytosis has been investigated by using various model systems and experimental approaches. In terms of model systems, this field has primarily relied on preparations derived from explanted organs rather than cell cultures. Indeed, cells isolated from exocrine organs and cultured on solid substrates rapidly dedifferentiate and within a few hours lose their polarity and secretory granules [23]. Instead, intact acinar preparations from pancreas, lacrimal glands, and SGs have been quite successful models and provided groundbreaking information on the kinetics of exocytosis and the molecular components regulating this process [11, 24]. In addition, lobule preparations and tissue slices have also been extensively used as model systems. The former, developed in David Castle's lab, have been instrumental in elucidating the complex nature of the secretory pathways in SGs, leading to the discovery of the minor regulated pathways [25, 26]. The latter, originally developed and used in the neurosciences, have been particularly useful for studying multiple aspects of regulated exocytosis both in the pancreas and in SGs [27, 28]. In these systems cell architecture is preserved compared to the native tissue since they retain several structural components, such as extracellular matrix, surrounding supporting cells, and ductal structures. Finally, regulated exocytosis has been studied in live rodents, although to a limited extent, due to challenges in the ability to manipulate these models [29].

In terms of experimental approaches, regulated exocytosis has been primarily investigated through the use of biochemical, immunological, or electrochemical assays. Although these methods permit an accurate determination of the amount of secreted molecules per cell, they do not reveal any information on the exocytic steps or the morphology and fate of individual exocytic vesicles. In this respect, assays based on measurements of membrane capacitance have provided detailed information on single fusion events at the plasma membrane, with the caveat of the inability to distinguish between endocytic and exocytic events. Electron microscopy has also been used to characterize the structure of the secretory granules at the plasma membrane before and after the fusion steps.

Finally, time-lapse light microscopy has elucidated several aspects of the dynamics of exocytosis in exocrine glands. Several studies were performed by bathing ex vivo preparations in small fluorescent dyes, such as sulforhodamine B or lucifer yellow, which accumulate in the ducts and upon the opening of the fusion pore access the lumen of the secretory granules. This approach has revealed that in most exocrine glands, secretory granules primarily undergo compound exocytosis [11, 14, 30–33]. Furthermore, it enabled measuring the kinetics of the pore expansion and the diffusion of proteins and lipids from the PM into the membrane of the granules [15, 34, 35]. More recently, laser-spinning disk has been

successfully used in isolated pancreatic acini where the exocytosis of large secretory granules containing the cargo molecule syncollin fused with the pH-sensitive fluorescent dye pHluorin has been studied under both physiological and pathological conditions [36].

2 Materials

2.1 Microscope and Preparation of the Stage

To image the SGs in live rats and mice, we used an inverted microscope (Olympus IX81 equipped with a Fluoview 1000 scanner [37]). The stage was equipped with an insert designed to accommodate a 35-mm petri dishes (Olympus America, Center Valley, PA) that was closed with a 40-mm glass coverslip (# 1.5, from Bioptechs, Butler, PA). To image regulated exocytosis, we used either a Plan-Apo 60x/1.2 NA water-immersion objective or a Plan-Apo 60x/1.42 NA oil objective (Olympus). The objectives were connected to an objective heater (Bioptechs, Butler, PA), whereas the stage was preheated with heated pads (Foot Warmers, Heat Factory, Vista, CA). Confocal microscopy was performed by exciting the fluorophores as follows: 488 nm for GFP (0.5–1 % laser power); 561 nm for td-Tomato, Texas Red, and Alexa 594 (10 % laser power); and 633 nm for Alexa 647 (20–25 % laser power). We mostly used scanning speeds ranging from 200 ms up to 1 s per frame. When high spatial and temporal resolution scans are required, high zoom of the scan area is used. For example, using a 60× objective, a 16× scan area zoom, and 128 × 128 pixel image will yield 0.103 μm/pixel spatial scale. With these settings, when pixel dwell time is set to 4 μs/pixel, the resultant scan speed is close to 200 ms per frame.

2.2 Animal Preparations

For intravital microscopy we use Sprague–Dawley rats (150–250 g, Harlan Laboratories, Frederick, MD), FVB mice expressing EGFP (GFP mice), and C57BL/6 mice expressing the membrane-targeted td-Tomato peptide (mTomato mice). Both transgenic lines were purchased from the Jackson Laboratory and bred as homozygous in the local animal facility. The optimal weight for imaging is 20–25 g. The first step in imaging the dynamics of regulated exocytosis in vivo is the preparation of the animals. Mice and rats need to acclimate for 2–3 days in the area where they are going to be imaged, since any sudden change in the environment results in various degrees of degranulation, as reported by others [38]. Interestingly, regardless of the dietary regimen (fed ad libitum or fasting), the number of the secretory granules is not significantly affected. Although we did not observe any difference in secretory response related to the gender of the animals, we perform all the experiments using male mice or rats.

However, it is crucial to minimize any distress related to the anesthesia. To this aim, we devised a procedure that involves the preinduction of anesthesia by using isoflurane inhalation in a vaporizer chamber (Braintree Scientific, Braintree, MA, 800–900 mmHg oxygen, 2–3 % isoflurane) followed by the intraperitoneal injection of a freshly prepared mixture of ketamine and xylazine (100 mg/kg and 20 mg/kg, respectively, using a 25-gauge needle). After the animals are anesthetized, particular care has to be taken to maintain the body temperature in a range between 35 and 38 °C. The temperature is constantly measured by using a rectal thermometer (MicroTherma 2 T Thermometer with RET-3 and IT-21 thermocouple probes, Braintree Scientific, Braintree, MA), and it is maintained by using heated pads (Foot Warmers, Heat Factory, Vista, CA) or heated lamps (model HL1, Braintree Scientific, Braintree, MA).

2.3 Surgical Procedures to Expose the Submandibular Salivary Glands and Positioning on the Microscope Stage

The neck area of the anesthetized animal was cleaned with a gauze sponge soaked in 70 % ethanol. A small piece of skin at the midline was lifted up with dull tweezers and cut with clean scissors (0.5–1 cm). The skin was moved away from the underlying tissue and excised in order to leave a 0.5-cm-wide and 2-cm-long opening. The connective tissue was separated away from the submandibular gland that is then constantly washed with saline or covered with optical coupling gel to prevent dehydration (see [39, 40]). The animal was positioned on its side onto the preheated stage with the exposed salivary gland placed in the center of the coverslip. Before proceeding with the immobilization of the gland, the animal was secured and stabilized in this position by using masking tape. A small piece of lens cleaning tissue was then sandwiched between the gland and a small plastic square that was gently pressed to stabilize the gland. Particular care was taken to ensure that the blood flow was properly maintained. To this aim, the blood and the extent of the motion were quickly evaluated by using epi-fluorescence microscopy. Once the proper stabilization was achieved, the plastic square was secured to the stage using masking tape.

2.4 Retro-Diffusion of Fluorescent Dyes into the Wharton's Duct

The anesthetized animal was secured into a previously described stereotactic device [39] with the mandibles wide open and the cheeks extended to the sides. The tongue was folded towards the back of the mouth to expose the ductal orifices without obstructing the airways. The stereotactic device was held at about 45° and positioned under a stereomicroscope (SZX7, Olympus America, Center Valley, PA) to visualize the area below the tongue and locate the two orifices of the Wharton's ducts. A 30–40-cm PE-5 cannula (Strategic Applications, Libertyville, IL) was gently pushed into the orifice and introduced into the duct using bent sharp tweezers. For mice, the cannula was thinned by carefully stretching it close to the open flame of a Bunsen burner. To seal the

cannula a small drop of Histoacryl tissue glue was applied to the orifice. The cannula was connected to a 1-ml syringe (via a 30- or a 33-GG needle), which contains the fluorescent dye (1–10 μg/ml in saline) and placed 25–30 cm above the animal to allow diffusion by gravity. After 20 min the acinar canaliculi should be clearly highlighted and visible by using epi-fluorescence microscopy. If not, a slight pressure can be applied to the plunger of the syringe to force the diffusion of the dye, but care must be taken to not disrupt the epithelial integrity.

3 Methods

3.1 Intravital Microscopy Permits the Visualization of Subcellular Structures In Vivo

Time-lapse light microscopy and the development of GFP technology have contributed to significant breakthroughs in understanding the dynamics and the mechanisms of several membrane-trafficking events, including regulated exocytosis. However, light microscopy has been primarily applied to in vitro and ex vivo models. In the early nineties, the development of two-photon microscopy [41] made deep tissue imaging possible and opened the door for the establishment of a new field called intravital microscopy (IVM). IVM has enabled imaging biological processes in several multicellular organisms, including rodents [42]. Initially, IVM has been applied primarily in the neurosciences to study synaptic plasticity and calcium signaling [43]. Afterwards, IVM was used to image the dynamics of cells involved in the immune response [44, 45] or to investigate cell migration and lympho-angiogenesis in tumor models [46–48]. Only recently, IVM has been applied to study the dynamics of subcellular structures in live animals. Indeed, the endocytosis of fluorescently labeled dextrans and folate has been imaged in the kidney of live rats and mice [49, 50].

Our group has developed a robust system to study membrane trafficking in vivo in live rodents using IVM. The ability to stabilize the SGs preparation, and minimizing motion artifacts due to heartbeat and respiration, combined with the use of selected transgenic mouse models has enabled us to investigate in detail the modality and the kinetics of regulated exocytosis in vivo [12, 13, 17, 51, 52]. We have also been able to study the endocytosis of selected molecules in rodent SGs and to follow their trafficking through the endo-lysosomal systems [40]. Furthermore, we have investigated the dynamics and modality of the internalization of naked DNA from the apical surface of the SG epithelium [18, 53]. Here, we provide a summary of the methods and tools that we have developed to carry out these studies. Since a detailed description of the procedures for animal handling has been recently published [39], we will focus primarily on the description of the models and the quantitative aspects of this approach.

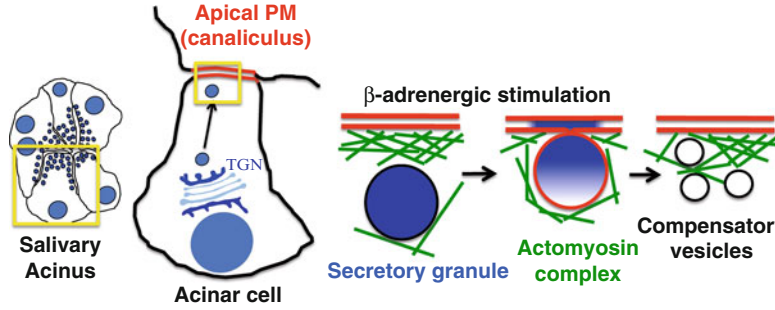

Fig. 1 Regulated exocytosis in salivary glands. In SGs, acini are the major secretory units and are composed of 9–10 polarized acinar cells [13]. The apical plasma membranes of adjacent acinar cells form the acinar canaliculi, which are very narrow ducts (0.3–0.4 μm in diameter) where both proteins and fluid are secreted. Secretory granules containing salivary proteins are formed from the trans-Golgi network and are transported to the apical plasma membrane. In resting conditions, secretory granules are prevented to fuse with the plasma membrane by a thick F-actin meshwork that acts as a functional barrier [2]. In both parotid and submandibular glands, the stimulation with beta-adrenergic receptor elicits docking and fusion of the secretory granules with the plasma membrane, the opening of the fusion pore, and the release of the cargo molecules into the canaliculi. The membranes of the secretory granules are first integrated in the apical plasma membrane via a process that requires the assembly of an actomyosin complex and successively retrieved by compensatory endocytosis

3.2 Tools and Procedures to Image the Secretory Granules at the Apical Plasma Membrane in the Salivary Glands of Live Rodents

In SGs, regulated exocytosis occurs primarily in the acini that are formed by polarized epithelial cells. Secretory granules are transported to the apical plasma membrane, where they fuse upon stimulation of the appropriate G protein-coupled receptor (Fig. 1). In order to investigate regulated exocytosis in vivo, we have developed a series of complementary approaches that make possible the visualization of the secretory granules, the apical plasma membrane, and other molecules that are implicated in this process. Specifically, these approaches are geared towards the elucidation of the steps that occur after the membrane bilayer of a secretory granule fuses with that of the plasma membrane.

In rodents, there are three major SGs: the parotid, which secretes primarily digestive enzymes, such as amylase; the submandibular, which secretes several molecules involved in defense against pathogens, such as peroxidase, lactoferrin, and immunoglobulins; and finally, the sublingual glands, which secrete primarily mucins [23]. In both the parotid and submandibular glands, regulated exocytosis is triggered by the stimulation of beta-adrenergic receptors, whereas in the sublingual gland, it is triggered by muscarinic stimulation [23]. As a model to study exocytosis, we selected the submandibular glands for two main reasons: first, they are located in the neck area and can be easily exposed and immobilized

to minimize the motion artifacts, as previously described [39, 40], and second, the excretory duct of the submandibular glands (Wharton's duct) is easily accessible and can be used to inject fluorescent molecules, pharmacological agents, or to transfect genes [18], whereas the parotid excretory duct (Stensen's duct) is not.

3.3 The GFP Mouse as a Model to Quantitatively Study Regulated Exocytosis

To visualize the secretory granules, we used a mouse strain (FVB) that expresses GFP in the cytoplasm and in the nuclei (GFP mouse) [13, 54]. After translation, GFP is not imported into the ER and thus is excluded from the lumen of most of the organelles in the secretory pathway. For this reason, in the acini of the submandibular glands, large structures, such as the secretory granules, appear as well-defined circular profiles that can be easily visualized by either two-photon (not shown) or confocal microscopy (Fig. 2b, arrows). Since the average diameter of the secretory granules is 1.5 μm (Fig. 2c), they can be optimally resolved by using confocal microscopy and adjusting the size of the pinhole (0.8–0.9 μm), as previously reported [13, 39]. Only a small percentage of the structures that exclude GFP are mitochondria or lysosomes that can be identified by using specific vital dyes such as mitotracker (Fig. 2d) and lysotracker (not shown). This is further confirmed by the fact that stimulating exocytosis with subcutaneous (SC) injections of isoproterenol significantly reduces the number of structures, which exclude the GFP (Fig. 2e).

In order to visualize the exocytic events, it is essential to first locate the apical plasma membrane (or canaliculi). In the GFP mouse canaliculi can be identified since they have some unique characteristics, such as the following: (1) They are shared by two acinar cells, (2) they exhibit an enrichment in the GFP levels that correlate with the enrichment in F-actin, and (3) they are surrounded by secretory granules (Fig. 2b, arrowheads and insets). The best fields of view are usually 15–30 μm below the surface of the glands, as determined by visualizing the collagen fibers by second harmonic generation (Fig. 2a, between dotted lines). Once the optimal imaging area has been determined, time-lapse imaging is performed by setting the acquisition speed between 0.2 and 1 s/frame. A typical imaging session comprises 3–4 time-lapse sequences (10 min each) that are acquired in the same area. Under resting conditions secretory granules are stationary and exhibit minimal motion, whereas they slightly increase their mobility after 1 min from the SC injection of isoproterenol [13].

Due to the limit of resolution of light microscopy and to the small shifts in the *z*-axis that occur during imaging, the fusion between the secretory granules and the canaliculi cannot be directly imaged. However, post-fusion steps can be precisely monitored. Indeed, after fusion with the plasma membrane and the opening of the fusion pore, the secretory granules recruit an actomyosin scaffold that nonspecifically binds GFP and other cytoplasmic proteins [13].

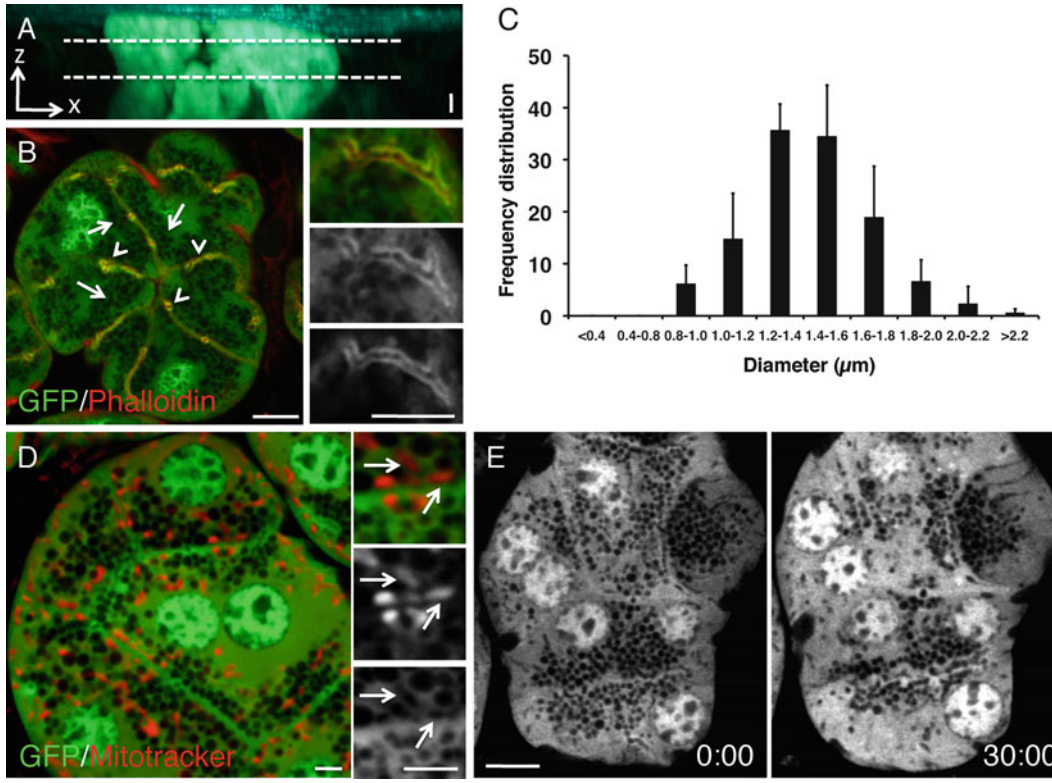

Fig. 2 Secretory granules visualized through the GFP mouse model. (**a**) The SGs of an anesthetized GFP mouse were exposed, and a Z-scan was performed by two-photon microscopy (excitation 930 nm, Plan-Apo 60x/1.2 NA water-immersion objective). The volume rendering was realized with Imaris (Bitplane), and the maximal projection of a side view (zx plane) is shown. Collagen fibers (cyan) appears in the first 2–5 μm from the surface of the tissue, and the two acini were fully reconstructed (*green*). Bar, 10 μm. (**b**, **c**) The SGs of a GFP mouse were excised and fixed with 2 % formaldehyde for 15 min. The glands were processed and labeled with Texas Red-phalloidin to reveal F-actin, as previously described [40]. The glands were imaged by confocal microscopy (excitation 488 and 561 nm, Plan-Apo 60x/1.4 NA oil objective). (**b**) Secretory granules appear as dark circular structures devoid of GFP (*arrows*) that are clustered around the F-actin-enriched canaliculi (*arrowheads*). Bar, 5 μm. *Insets*—High magnification of a canaliculus. Note the enrichment of both GFP (*middle panel*) and F-actin (*lower panel*) on the limiting membranes of the canaliculus. Bar, 5 μm. (**c**) For each acinus, the diameters of the secretory granules were measured manually, and their frequency distribution was calculated. Each bar represents the average frequency distribution for ten acini in the same animal (±SD). The measurements were repeated in four animals with similar results. (**d**, **e**) The SGs of anesthetized GFP mice were exposed and bathed for 20 min either with 500 nm of Far red-mitotracker (Invitrogen) (**d**) or with saline (**e**). (**d**) The SGs were imaged by confocal microscopy (excitation 488 and 647 nm). Mitochondria appear as elongated profiles (*arrows*). Bars, 3 μm. (**e**) The exposed SGs were imaged in time-lapse (excitation 488 nm, 1 frame/s), and 0.25 mg/kg of isoproterenol was injected SC to stimulate exocytosis. A snapshot was taken at time 0 and after 30 min from the injection. Note that the number of secretory granules is substantially reduced. Bar, 10 μm

This results in a sharp increase in the GFP levels around the limiting membranes of the secretory granules followed by a slow decline that mirrors their decrease in size (Fig. 3b, c). These "flashes of GFP" represent bona fide exocytic events since they are correlated with the

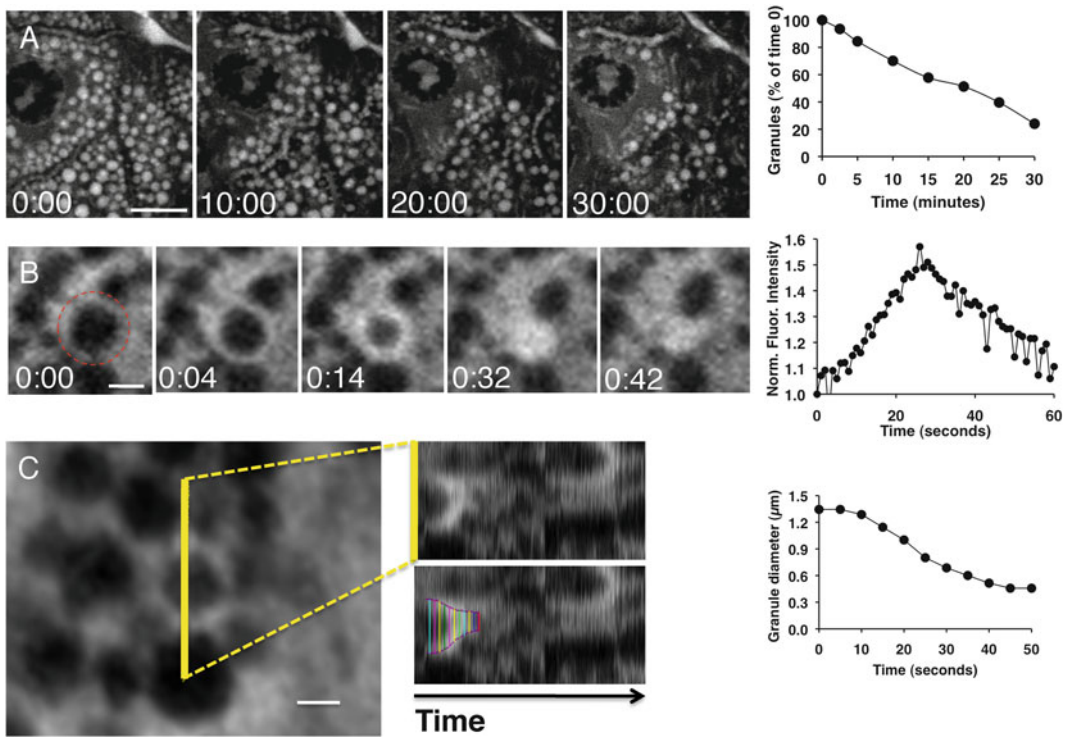

Fig. 3 Analysis of degranulation and lifetime of the secretory granules at the plasma membrane after fusion by using the GFP mouse. (**a–c**) The SGs of an anesthetized GFP mouse were exposed and imaged in time-lapse by confocal microscopy (excitation 488 nm, 1 frame/s). Isoproterenol (0.25 mg/Kg) was injected SC to stimulate exocytosis. Four movies, 10 min each, were acquired. (**a**) Frames at selected times were processed and used to score the number of secretory granules. Briefly, each frame was inverted by using Photoshop to highlight the secretory granules. Circular profiles larger than 800 nm were scored as secretory granules and reported as a function of time (graph on the right). Bar, 10 μm. (**b**, **c**) The movies were converted into time sequences by using Metamorph and analyzed to identify and select secretory granules close to the apical plasma membrane that exhibited an increase in the intensity of the GFP fluorescence around their limiting membranes. If needed, any shift in the xy plane was corrected by processing the time sequence with ImageJ (Stag-reg plug-ins). Importantly, time sequences with major shifts along the *z*-axis were not used for the analysis. A region of interest was drawn around the selected granule (**b**, *red broken circle*) or a line parallel to the apical pole (**c**, *yellow solid line*). The region measurement (**b**) or the kymograph (**c**) functions were used to record the integrated fluorescence intensity (IFI) or determine the diameter for each time frame, respectively (see Section 3). Representative curves are shown for a single granule. In a typical experiment 10–15 granules per acinus are evaluated and 3–4 animals per condition are used. Bars, 1 μm

decreasing number of secretory granules per acinar cell, as previously shown [13].

In order to characterize this process, we quantitatively evaluate three parameters: the extent of degranulation, the intensity of the GFP around individual granules, and their diameters over time. First, the time-lapse sequences are processed with ImageJ (StackReg plug-in) to correct for any slight shift in xy due to residual motion artifacts. In order to estimate the extent of degranulation, a

minimum of 6 frames are selected: the first frame right after the injection of isoproterenol (time 0) and the others after 2.5, 5, 10, 20, and 30 min (Fig. 3a). The frames are processed with Photoshop, converted to grayscale mode, and inverted to highlight the secretory granules (Fig. 3a). All vesicular profiles with a diameter above 800 nm are scored as secretory granules, normalized to the number of granules at time 0, and reported as % of granules versus time (Fig. 3a, graph). This approach provides information on the kinetics of degranulation of the secretory granules and can be used to study several aspects of the mechanisms controlling regulated exocytosis. For example, we characterized the optimal doses of isoproterenol and showed that muscarinic stimulation does not elicit any exocytic events in vivo in the submandibular glands [13]. Moreover, this method can be coupled with the administration of pharmacological agents in order to dissect the molecular machinery that regulates this process.

Measuring both the GFP levels around the secretory granules and their diameter provides information on their lifetime after fusion with the plasma membrane. The GFP levels can be measured using Metamorph (Molecular Devices, Sunnyvale, CA). Specifically, a region of interest is drawn around each individual granule (Fig. 3b, red broken circle), and the integrated fluorescent intensity (IFI) is recorded for each time point by using the region measurement function. The value of IFI recorded 5 s before the sharp increase of the GFP levels is used as a baseline for the normalization. As for the measurement of the diameter of the secretory granules over time, we used the kymograph function of Metamorph. A line parallel to the apical plasma membrane is drawn across the diameter of an individual secretory granule, and a kymograph is generated, as shown in Fig. 3c. The diameters are then outlined manually in the kymograph at selected time points, measured, and reported as a function of time. Based on these measurements, we estimated that after fusion with the plasma membranes, the secretory granules last 40–60 s and undergo a gradual collapse [13]. An important remark is that although this process is relatively slow and can be fully documented by acquiring the time-lapses at a lower scan speed, we still recommend a slight oversampling to compensate for the small drifts in the *z*-axis that occasionally occur.

This mouse model provides invaluable information on regulated exocytosis in vivo, and it can be also used to study other exocrine glands, such as the pancreas, lacrimal glands, and mammary glands. However, it is not a viable option to study endocrine glands, such as endocrine pancreas and adrenal medulla, or neurons, since in these organs the size of the secretory vesicles are close to the limit of resolution of light microscopy and the exocytic events occur on the order of milliseconds.

3.4 The mTomato Mouse as a Model to Visualize the Apical Plasma Membrane During Regulated Exocytosis

To visualize the apical plasma membrane during regulated exocytosis, we used a mouse that expresses a membrane-targeted peptide fused with the fluorescent protein tandem-Tomato (mTomato mouse). This peptide is derived from the first 8 N-terminal amino acids of MARCKS (myristoylated alanine-rich kinase substrate), and it is myristoylated on the first methionine and palmitoylated at the cysteine in position 3 and 4 [55]. In SGs, the peptide is localized both at the basolateral and the apical plasma membrane, but it is not present on secretory granules or on any other intracellular organelle (Fig. 4a) [13]. Canaliculi can be easily identified when they are oriented in parallel (Fig. 4a, asterisk) or perpendicularly (4A, arrows) to the xy plane. This mouse model enables imaging the secretory granules after fusion with the plasma membrane since the fluorescent peptide diffuses into their limiting membranes (Fig. 4a, asterisks). Moreover, this mouse model permits us to visualize the morphological changes of the apical plasma membranes upon its integration with the membrane of each secretory granule, as shown by the large expansion in the diameter of the canaliculi (Fig. 4a, arrows). The advantage of this model versus the GFP mouse is the fact that only granules fused with the plasma membrane are visualized. This model was instrumental in confirming that in SGs in vivo regulated exocytosis occurs primarily via single fusion events rather than compound exocytosis [12, 13].

The kinetics of the gradual collapse of the secretory granules can be determined by measuring the fluorescence intensity of the td-Tomato peptide, as soon as it appears in the limiting membranes of the granules. Similarly to what has been shown for the GFP mouse, a region of interest is drawn around the secretory granules,

Fig. 4 (continued) stimulate exocytosis. Six movies, 10 min each, were acquired. (**a**) The fluorescent peptide is localized at the cell surface of the acini. The apical canaliculi can be easily identified for their peculiar morphology particularly when they are oriented perpendicularly to the xy plane. Indeed, they appear as small circular profiles that expand after stimulation of exocytosis (*arrows*). When the canaliculi are oriented in parallel to the xy plane, they are more difficult to identify and appear visible only after they enlarge or when secretory granules are observed after fusion (*asterisk*). Bars, 10 μm. (**b**, **c**) The movies were converted into time sequences by using Metamorph, corrected for shift in the xy plane (ImageJ, Stag-reg plug-ins), and analyzed to identify the apical pole and the sites where exocytosis occurs. (**b**) Three frames were processed to show the expansion of the apical plasma membrane (*arrows*) and a secretory granule after fusion (*arrowhead*). Bar, 5 μm. (**c**) A region of interest was drawn around the granules after the fluorescent peptide diffused from the apical plasma membrane (**b**, *dotted red line*) or a line parallel to the plasma membrane (**c**, *solid yellow line*). The region measurement (**b**) or the kymograph (**c**) functions were used to record the integrated fluorescence intensity (IFI) or determine the diameter for each time frame, respectively (see Section 3). Notably, the kinetics of collapse of the secretory granules were in agreement with the kinetics determined using the GFP mouse (Fig. 3). In a typical experiment 10–15 granules per acinus are evaluated, and 3–4 animals per condition are used. Bars, 1 μm. (**d**) Large vacuoles derived from the secretory granules fused at the plasma membrane were detected inside acinar cells. The diameter of the granules was determined as described above and reported as a function of time. Bar, 1 μm

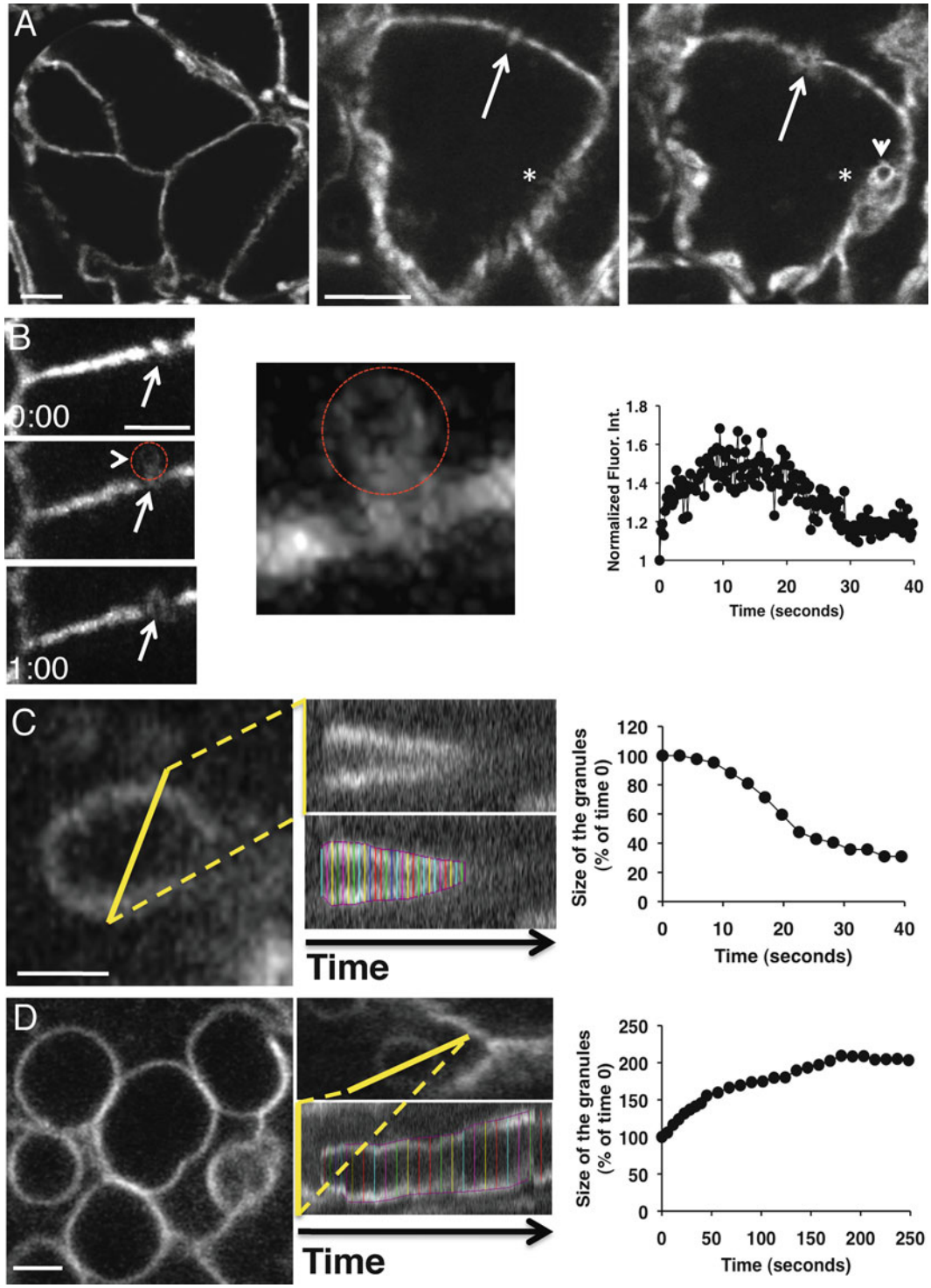

Fig. 4 Imaging the apical plasma membrane and the lifetime of the secretory granules by using the mTomato mouse. (**a–d**) mTomato mice were anesthetized, the SGs were exposed and either incubated with saline (**a**–**c**) or bathed in 10 μm cytochalasin D (**d**) as described in [13]. The SGs were imaged by using time-lapse confocal microscopy (excitation 561 nm, 200 ms/frame). After 20 min isoproterenol (0.25 mg/Kg) was injected SC to

and the IFI is recorded by using Metamorph (Fig. 4b, red broken circle). Alternatively, these kinetics can be studied by using kymographs to measure the diameter of the secretory granules (Fig. 3c). Notably, the kinetics of the gradual collapse determined with these methods are consistent with those determined using the GFP-mouse (Fig. 4c), indicating that the expression of these two reporter transgenes does not affect the dynamics of the process.

This approach is particularly useful to identify molecules that may regulate post-fusion events. For example, the role of the actin cytoskeleton in this process can be highlighted by administering actin-disrupting agents, such as latrunculin A or cytochalasin D. These drugs can be administered using several routes, such as bathing the glands on the microscope stage [13], retro-diffusion by injection through the salivary duct [40], or intra-organ injections. The optimal method may have to be determined by the investigator depending on the experimental conditions. The main effect of disrupting the actin cytoskeleton is to block the gradual collapse of the secretory granules, which instead progressively enlarge to form large vacuolar structures connected to the apical plasma membrane (Fig. 4d). The kymograph-based measurements of the granule diameters have revealed that the expansion of the secretory granules is a two-step process (Fig. 4d). Based on this finding, we performed a more detailed analysis and showed that the increase in size of the granules is initially due to the hydrostatic pressure generated by the secretion of fluids inside the canaliculi and later due to the fusion of other secretory granules with those that are already fused at the plasma membrane [12, 13].

This mouse provides invaluable information on several aspects of regulated exocytosis, such as the fate of the individual granules after fusion with the plasma membrane, the organization of the apical plasma membrane, and some biophysical properties of the membranes such as membrane mobility (graph in Fig. 4b). It is important to emphasize that the td-Tomato peptide is localized primarily at the cell surface and it is not enriched in the secretory granules or any other intracellular organelles before or after stimulation. This prevents the use of this mouse model to investigate the biophysical properties of the secretory granules before fusion or to study compensatory endocytosis.

3.5 Retro-Diffusion of Fluorescent Dyes in the Salivary Ducts to Monitor the Opening of the Fusion Pore and Compensatory Endocytosis

One of the main methods to study regulated exocytosis in ex vivo preparations from exocrine glands is to bathe the tissue in small fluorescent molecules such as lucifer yellow, sulforhodamine B, or low molecular weight dextrans [11, 24]. These dyes fill the ducts and the apical canaliculi and access the lumen of the granules upon the opening of the fusion pore. Moreover, this approach has been used to determine the size of the fusion pore by using probes with a known stokes radius, such as large molecular weight dextrans [21, 56]. In order to adapt this method to live animals, we introduced

fine polyethylene cannulae into the Wharton's duct of anesthetized rats and used them to deliver fluorescent molecules to the acinar canaliculi [18, 40]. Since very small molecules have been shown to rapidly diffuse through the tight junctions in the SG epithelium [57], we routinely use 10 kDa dextran that has a relatively large stokes radius, and it is almost completely retained in the ducts.

After the submandibular SGs are surgically exposed, the anesthetized animals are placed on the microscope stage, and the dyes are allowed to slowly diffuse by gravity into the large ducts and the small acinar canaliculi [13]. After 20 min the acinar canaliculi are clearly visible, and after the identification of the appropriate imaging area, isoproterenol (0.1–0.25 mg/kg) is injected SC. It is important to emphasize that in order to detect the opening of the fusion pore and to monitor the influx of the dye, the acquisition speed has to be set to a minimum of 200–300 ms/frame (or higher depending on the instrumentation). After approximately 1 min, the dye appears inside the lumen of the secretory granules at the apical plasma membrane. As observed before, the secretory granules undergo a gradual collapse. Both the IFI and the diameter of the secretory granules can be measured as described in Fig. 3 and 4 showing that the kinetics of the gradual collapse in live rats is very similar to that measured in mice using the transgenic models (Fig. 5b graph).

Notably, this approach can be also used to image compensatory endocytosis, as well. Indeed, after few minutes following stimulation of regulated exocytosis, several small vesicular structures derived from the apical plasma membrane [18] are observed in the cytoplasm of the acinar cells (Fig. 5c, arrowheads and insets). It is important to emphasize that since compensatory vesicles are smaller than secretory granules (approximately 100 nm) [18], the gain of the detectors has to be adjusted to detect smaller structures. This results in a slight saturation of the fluorescent signal in the canaliculi (Fig. 5c, left panel).

Unfortunately, a major limitation of this approach in live animals is the fact that the visualization of both the opening of the fusion pore and the formation of compensatory vesicles are restricted to the first few minutes from the onset of regulated exocytosis. This is because fluorescent dextrans are washed out from the canaliculi after 3–5 min following the injection of isoproterenol, as clearly observed by comparing the levels of dextran in the canaliculi before and after stimulation [18, 51]. Unfortunately, any attempt to diffuse or inject additional amounts of dyes results in the disruption of the epithelial integrity. Nonetheless, this approach provides a very powerful tool to characterize the machinery regulating both processes. Indeed, the retro-diffusion of the fluorescent dyes can be coupled to the use of pharmacological agents. Moreover, cannulae can be inserted in mice providing the opportunity to extend this method to the transgenic mice described above.

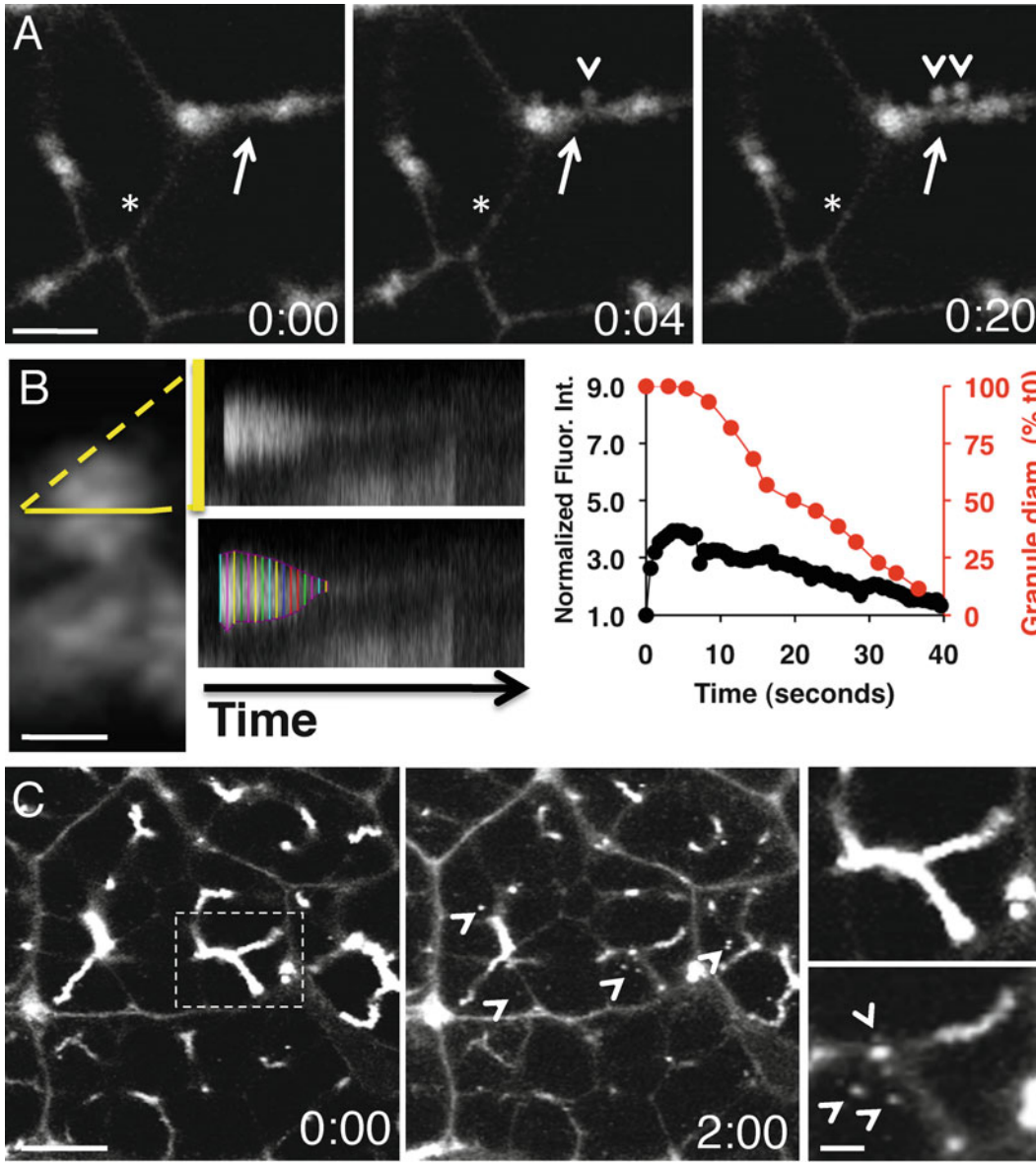

Fig. 5 Imaging the opening of the fusion pore and compensatory endocytosis by retro-diffusion of a fluorescent dye in the salivary ducts of live rats. (**a–c**) Sprague–Dawley rats were anesthetized, and a fine polyethylene cannula was inserted into the Wharton's duct. The SGs were exposed, and 10 μg/ml 10 kDa Texas Red dextran was retro-diffused by gravity as described in the Section 3. After 20 min the SGs were imaged by time-lapse confocal microscopy (excitation 561 nm, 200 ms/frame), and 0.25 mg/kg of isoproterenol was injected SC to stimulate exocytosis. (**a**) The acinar canaliculi are highlighted (*arrows*), and after the opening of the fusion pore, the fluorescent dextran accesses the lumen of the secretory granules (*arrowheads*). A small amount of dextran reaches the basolateral membrane (*asterisk*). Bar, 10 μm. (**b**) The IFI and diameter of the granules were determined as described in legends to Figs. 3 and 4. (**c**) After 2 min from the injection of isoproterenol, several small vesicles containing Texas Red dextran are observed in the cytoplasm of the acinar cells (*arrowheads* and *insets*). Note the reduction of the amount of dextran in the canaliculi, due to the secretion of fluids that wash out the dye. Bars, 10 μm and 1 μm (*insets*)

4 Conclusions

IVM has provided the means to investigate the dynamics of intracellular structures in live animals. Specifically, the combination of IVM with the ability to express or ablate genes in live animals has made possible addressing old and new questions in cell biology at a molecular level. Regulated exocytosis is a clear example of the full potential of this approach, as shown by the use of a series of selected transgenic mice (described here) and various tools, such as pharmacological agents and the transient expression of genes [18].

As for the mouse models, the GFP and mTomato strains have been instrumental in defining the general characteristics of regulated exocytosis in SGs in vivo such as regulation, rate of degranulation, modality of exocytosis (full collapse vs. compound exocytosis), and in providing a glimpse of the biophysical properties of the plasma membrane in vivo. We envision that these mice will be extremely valuable to characterize this process in other exocrine organs such as the pancreas, lacrimal glands, and mammary glands. In addition, the generation of new strains expressing either fluorescently tagged reporters for component of the actin cytoskeleton (e.g., Lifeact and myosin II) or Ca^{++} and cAMP sensors (e.g., Chameleon) will provide additional information on the integration between cell signaling and the cytoskeleton during regulated exocytosis. Moreover, further investigation may be possible by crossing these reporter mice with selected knockout animals.

The use of pharmacological agents and the expression of selected genes are also two very powerful tools. In this respect, the SGs represent an ideal organ due to the easy access through the oral cavity. Indeed, SGs have been used as a target organ to selectively deliver drugs, to express transgenes via non-viral- and viral-mediated approaches, and to acutely downregulate proteins via siRNA and shRNA. However, the development of novel and more sophisticated vehicles to accomplish tissue-specific targeting of molecules and genes will enable expanding this approach to the other exocrine organs.

In conclusion, we foresee that in the next few years, IVM will contribute to unraveling several molecular aspects of regulated exocytosis in the exocrine glands of live animals. This approach has the potential to be extended to other secretory organs, membrane-trafficking steps, and more broadly to other cell biological processes as well.

Acknowledgments

This research was supported by the Intramural Research Program of the NIH, National Institute of Dental, and Craniofacial Research.

References

1. Burgoyne RD, Morgan A (2003) Secretory granule exocytosis. Physiol Rev 83:581–632
2. Porat-Shliom N, Milberg O, Masedunskas A, Weigert R (2013) Multiple roles for the actin cytoskeleton during regulated exocytosis. Cell Mol Life Sci 70(12):2099–2121
3. Sudhof TC, Rizo J (2011) Synaptic vesicle exocytosis. Cold Spring Harb Perspect Biol 3
4. De Matteis MA, Luini A (2008) Exiting the golgi complex. Nat Rev Mol Cell Biol 9: 273–284
5. Luini A, Mironov AA, Polishchuk EV, Polishchuk RS (2008) Morphogenesis of post-Golgi transport carriers. Histochem Cell Biol 129:153–161
6. Parekh AB, Putney JW Jr (2005) Store-operated calcium channels. Physiol Rev 85:757–810
7. Petersen OH (2003) Localization and regulation of Ca2+ entry and exit pathways in exocrine gland cells. Cell Calcium 33:337–344
8. Seino S, Shibasaki T (2005) Pka-dependent and pka-independent pathways for camp-regulated exocytosis. Physiol Rev 85: 1303–1342
9. Hou JC, Min L, Pessin JE (2009) Insulin granule biogenesis, trafficking and exocytosis. Vitam Horm 80:473–506
10. Malacombe M, Bader MF, Gasman S (2006) Exocytosis in neuroendocrine cells: new tasks for actin. Biochim Biophys Acta 1763: 1175–1183
11. Kasai H, Kishimoto T, Nemoto T, Hatakeyama H, Liu TT, Takahashi N (2006) Two-photon excitation imaging of exocytosis and endocytosis and determination of their spatial organization. Adv Drug Deliv Rev 58:850–877
12. Masedunskas A, Porat-Shliom N, Weigert R (2012) Linking differences in membrane tension with the requirement for a contractile actomyosin scaffold during exocytosis in salivary glands. Commun Integr Biol 5:84–87
13. Masedunskas A, Sramkova M, Parente L et al (2011) Role for the actomyosin complex in regulated exocytosis revealed by intravital microscopy. Proc Natl Acad Sci U S A 108: 13552–13557
14. Pickett JA, Edwardson JM (2006) Compound exocytosis: mechanisms and functional significance. Traffic 7:109–116
15. Thorn P, Parker I (2005) Two phases of zymogen granule lifetime in mouse pancreas: Ghost granules linger after exocytosis of contents. J Physiol 563:433–442
16. Khandelwal P, Ruiz WG, Apodaca G (2010) Compensatory endocytosis in bladder umbrella cells occurs through an integrin-regulated and rhoa- and dynamin-dependent pathway. EMBO J 29:1961–1975
17. Masedunskas A, Sramkova M, Weigert R (2011) Homeostasis of the apical plasma membrane during regulated exocytosis in the salivary glands of live rodents. Bioarchitecture 1:225–229
18. Sramkova M, Masedunskas A, Parente L, Molinolo A, Weigert R (2009) Expression of plasmid DNA in the salivary gland epithelium: novel approaches to study dynamic cellular processes in live animals. Am J Physiol Cell Physiol 297:C1347–C1357
19. Jerdeva GV, Wu K, Yarber FA et al (2005) Actin and non-muscle myosin ii facilitate apical exocytosis of tear proteins in rabbit lacrimal acinar epithelial cells. J Cell Sci 118:4797–4812
20. Nightingale TD, Cutler DF, Cramer LP (2012) Actin coats and rings promote regulated exocytosis. Trends Cell Biol 22(6):329–337
21. Larina O, Bhat P, Pickett JA et al (2007) Dynamic regulation of the large exocytotic fusion pore in pancreatic acinar cells. Mol Biol Cell 18:3502–3511
22. Nemoto T, Kojima T, Oshima A, Bito H, Kasai H (2004) Stabilization of exocytosis by dynamic f-actin coating of zymogen granules in pancreatic acini. J Biol Chem 279:37544–37550
23. Gorr SU, Venkatesh SG, Darling DS (2005) Parotid secretory granules: crossroads of secretory pathways and protein storage. J Dent Res 84:500–509
24. Kasai H, Hatakeyama H, Kishimoto T, Liu TT, Nemoto T, Takahashi N (2005) A new quantitative (two-photon extracellular polar-tracer imaging-based quantification (tepiq)) analysis for diameters of exocytic vesicles and its application to mouse pancreatic islets. J Physiol 568: 891–903
25. Castle AM, Huang AY, Castle JD (2002) The minor regulated pathway, a rapid component of salivary secretion, may provide docking/fusion sites for granule exocytosis at the apical surface of acinar cells. J Cell Sci 115: 2963–2973
26. Castle JD (1998) Protein secretion by rat parotid acinar cells. Pathways and regulation. Ann N Y Acad Sci 842:115–124
27. Chen Y, Warner JD, Yule DI, Giovannucci DR (2005) Spatiotemporal analysis of exocytosis in mouse parotid acinar cells. Am J Physiol Cell Physiol 289:C1209–C1219

28. Warner JD, Peters CG, Saunders R et al (2008) Visualizing form and function in organotypic slices of the adult mouse parotid gland. Am J Physiol Gastrointest Liver Physiol 295: G629–G640
29. Proctor GB, Carpenter GH (2007) Regulation of salivary gland function by autonomic nerves. Auton Neurosci 133:3–18
30. Behrendorff N, Dolai S, Hong W, Gaisano HY, Thorn P (2011) Vesicle-associated membrane protein 8 (vamp8) is a snare (soluble n-ethylmaleimide-sensitive factor attachment protein receptor) selectively required for sequential granule-to-granule fusion. J Biol Chem 286:29627–29634
31. Nemoto T, Kimura R, Ito K et al (2001) Sequential-replenishment mechanism of exocytosis in pancreatic acini. Nat Cell Biol 3: 253–258
32. Segawa A, Riva A (1996) Dynamics of salivary secretion studied by confocal laser and scanning electron microscopy. Eur J Morphol 34: 215–219
33. Segawa A, Terakawa S, Yamashina S, Hopkins CR (1991) Exocytosis in living salivary glands: direct visualization by video-enhanced microscopy and confocal laser microscopy. Eur J Cell Biol 54:322–330
34. Pickett JA, Thorn P, Edwardson JM (2005) The plasma membrane q-snare syntaxin 2 enters the zymogen granule membrane during exocytosis in the pancreatic acinar cell. J Biol Chem 280:1506–1511
35. Thorn P, Fogarty KE, Parker I (2004) Zymogen granule exocytosis is characterized by long fusion pore openings and preservation of vesicle lipid identity. Proc Natl Acad Sci U S A 101:6774–6779
36. Fernandez NA, Liang T, Gaisano HY (2011) Live pancreatic acinar imaging of exocytosis using syncollin–phluorin. Am J Physiol Cell Physiol 300:C1513–C1523
37. Masedunskas A, Weigert R (2008) Internalization of fluorescent dextrans in the submandibular salivary glands of live animals: a study combining intravital two-photon microscopy and second harmonic generation. SPIE, In, pp 68601V–68612V
38. Peter B, Van Waarde MA, Vissink A, s-Gravenmade EJ, Konings AW (1995) Degranulation of rat salivary glands following treatment with receptor-selective agonists. Clin Exp Pharmacol Physiol 22:330–336
39. Masedunskas A, Sramkova M, Parente L, Weigert R (2013) Intravital microscopy to image membrane traffickingin live rats Cell imaging techniques. Methods Mol Biol 931: 153–167
40. Masedunskas A, Weigert R (2008) Intravital two-photon microscopy for studying the uptake and trafficking of fluorescently conjugated molecules in live rodents. Traffic 9:1801–1810
41. Zipfel WR, Williams RM, Webb WW (2003) Nonlinear magic: multiphoton microscopy in the biosciences. Nat Biotechnol 21:1369–1377
42. Weigert R, Sramkova M, Parente L, Amornphimoltham P, Masedunskas A (2010) Intravital microscopy: a novel tool to study cell biology in living animals. Histochem Cell Biol 133:481–491
43. Svoboda K, Yasuda R (2006) Principles of two-photon excitation microscopy and its applications to neuroscience. Neuron 50:823–839
44. Cahalan MD, Parker I (2008) Choreography of cell motility and interaction dynamics imaged by two-photon microscopy in lymphoid organs. Annu Rev Immunol 26:585–626
45. Germain RN, Castellino F, Chieppa M et al (2005) An extended vision for dynamic high-resolution intravital immune imaging. Semin Immunol 17:431–441
46. Alexander S, Koehl GE, Hirschberg M, Geissler EK, Friedl P (2008) Dynamic imaging of cancer growth and invasion: a modified skin-fold chamber model. Histochem Cell Biol 130: 1147–1154
47. Amornphimoltham P, Masedunskas A, Weigert R (2011) Intravital microscopy as a tool to study drug delivery in preclinical studies. Adv Drug Deliv Rev 63:119–128
48. Ritsma L, Ponsioen B, van Rheenen J (2012) Intravital imaging of cell signaling in mice. Intravital 1:2–10
49. Dunn KW, Sandoval RM, Kelly KJ et al (2002) Functional studies of the kidney of living animals using multicolor two-photon microscopy. Am J Physiol Cell Physiol 283:C905–C916
50. Sandoval RM, Kennedy MD, Low PS, Molitoris BA (2004) Uptake and trafficking of fluorescent conjugates of folic acid in intact kidney determined using intravital two-photon microscopy. Am J Physiol Cell Physiol 287: C517–C526
51. Masedunskas A, Milberg O, Porat-Shliom N et al (2012) Intravital microscopy: a practical guide on imaging intracellular structures in live animals. Bioarchitecture 2
52. Masedunskas A, Porat-Shliom N, Weigert R (2012) Regulated exocytosis: novel insights from intravital microscopy. Traffic 13:627–634

53. Sramkova M, Masedunskas A, Weigert R (2012) Plasmid DNA is internalized from the apical plasma membrane of the salivary gland epithelium in live animals. Histochem Cell Biol 138(2):201–213
54. Hadjantonakis AK, Gertsenstein M, Ikawa M, Okabe M, Nagy A (1998) Generating green fluorescent mice by germline transmission of green fluorescent es cells. Mech Dev 76: 79–90
55. Muzumdar MD, Tasic B, Miyamichi K, Li L, Luo L (2007) A global double-fluorescent cre reporter mouse. Genesis 45:593–605
56. Bhat P, Thorn P (2009) Myosin 2 maintains an open exocytic fusion pore in secretory epithelial cells. Mol Biol Cell 20:1795–1803
57. Mazariegos MR, Tice LW, Hand AR (1984) Alteration of tight junctional permeability in the rat parotid gland after isoproterenol stimulation. J Cell Biol 98:1865–1877